From the multibaker map to the fluctuation theorem for currents

Center for Nonlinear Phenomena and Complex Systems,
Université Libre de Bruxelles, Campus Plaine, Code Postal 231,
B-1050 Brussels, Belgium.
Pierre Gaspard[1]
David Andrieux[2]

Abstract. An overview is given of work carried out in collaboration with late Professor Shuichi Tasaki on the multibaker map. In this collaboration, the nonequilibrium steady states and the diffusive modes of this model of deterministic diffusion were shown to be described by distributions that are expressed in terms of the nondifferentiable Takagi and de Rham functions, respectively. The link to more recent work is established with a proof of a fluctuation theorem for the current flowing across a multibaker chain connected to two reservoirs.

1 Introduction

This article is dedicated to the memory of Professor Shuichi Tasaki (1958-2010) with whom a fruitful collaboration was in progress since 1993 until he unexpectedly passed away the 6th of June 2010. This collaboration started with a study of the nonequilibrium steady states and the relaxation modes of the multibaker map [1, 2, 3], which is an exactly solvable model of deterministic diffusion [4]. Its dynamics is chaotic as it is the case in the hard-disk Lorentz gas [5, 6]. In spite of this complexity and thanks to the piecewise-linear form of the map, the programme of nonequilibrium statistical mechanics can be carried out in full mathematical terms for the multibaker model. This programme consists in solving the Liouvillian time evolution of statistical ensembles of particles or trajectories transported by the Hamiltonian dynamics of the map.

In this framework, we could construct the nonequilibrium steady states and the relaxation modes of the multibaker as the eigenstates of the Liouvillian dynamics associated with the corresponding eigenvalues known as Pollicott-Ruelle resonances [7, 8, 9, 10]. These eigenstates turn out to be given by distributions that are singular with respect to Lebesgue's measure and

[1]E-mail: gaspard@ulb.ac.be
[2]E-mail: david.andrieux@ulb.ac.be

showing fractal-like features [1, 2, 3]. In this way, a new class of fractal objects were discovered, which play a fundamental role in nonequilibrium statistical mechanics. In particular, these distributions explicitly show how the time-reversal symmetry is broken at the statistical level of description. Moreover, these studies confirmed the central role of dynamical large-deviation properties that were previously considered in chaos theory [11] and thereafter introduced in nonequilibrium statistical mechanics [12, 13, 14, 15, 16, 17]. Recently, our collaboration with late Shuichi Tasaki concerned the quantum fluctuation theorem for the currents crossing nanodevices such as quantum dots or quantum coherent conductors, a topic which has recently known major developments [18, 19, 20, 21, 22, 23, 24].

The purpose of the present paper is to give an overview of the advances carried out in collaboration with late Professor Tasaki from the mathematical resolution of the Liouvillian dynamics of the multibaker map [1, 2, 3] until the quantum fluctuation theorem published in 2009 [20]. With the aim to establish the link between both contributions, we show that the multibaker map obeys a current fluctuation theorem holding under nonequilibrium steady conditions.

The paper is organized as follows. The multibaker map is presented in Section 2. The mathematical construction of its nonequilibrium steady states and its relaxation modes is reviewed in Sections 3 and 4. Section 5 is devoted to a discussion of the time-reversal symmetry breaking as revealed by the analysis. In Section 6, the current fluctuation theorem is obtained for the multibaker map, which establishes the link with recent work. Conclusions are drawn in Section 7.

2 The multibaker map

2.1 The infinite multibaker map

The multibaker map can be considered as a simplification of the Poincaré-Birkhoff map in the hard-disk Lorentz gas [5]. In Lorentz gases, independent particles move in a spatially-periodic potential formed by a lattice of immobile obstacles. Lorentz gases are classical models of electron transport in crystals where the obstacles are the ions. Since the pioneering work by Lorentz in 1905 [25], different types of obstacles have been envisaged such as hard disks or screened Coulomb potentials [26, 27]. For such obstacles, the classical dynamics is known to be chaotic (see Fig. 1). The continuous-time dynamics is reduced to a discrete-time map with a Poincaré surface of section intersecting the trajectories of the flow. In the case of the hard-disk Lorentz gas, the natural surface of section corresponds to the place where the particles bounce on the disks. As in other billiards, Birkhoff coordinates can be introduced as the arc of perimeter of the wall and the sine of the angle between the outgoing velocity and the normal to the wall at the point where the particle bounces [5]. In this way, a mapping is defined which describes

the bouncing ball dynamics from disk to disk across the lattice. The resulting map is area-preserving and has the main features of hyperbolic maps. However, the Poincaré-Birkhoff map of the hard-disk Lorentz gas is too complicated for the Liouvillian time evolution to be exactly solvable.

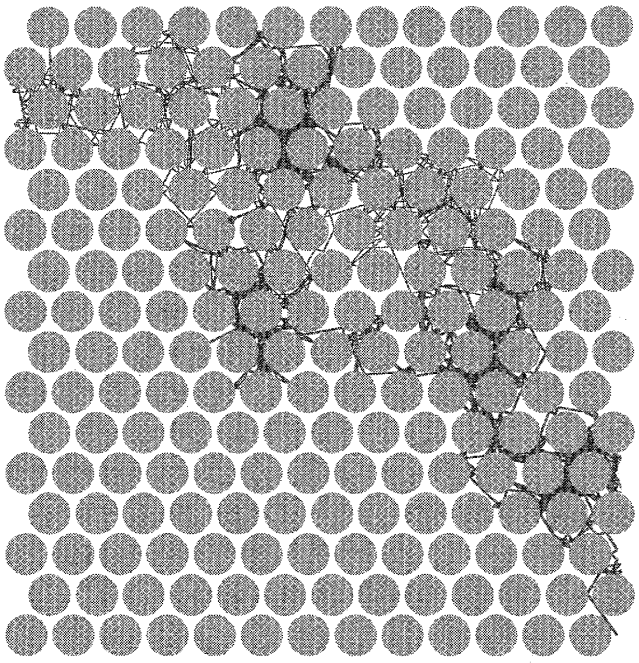

Figure 1: Hard-disk Lorentz gas with two trajectories starting from the same position but velocities which differ by one part in a million.

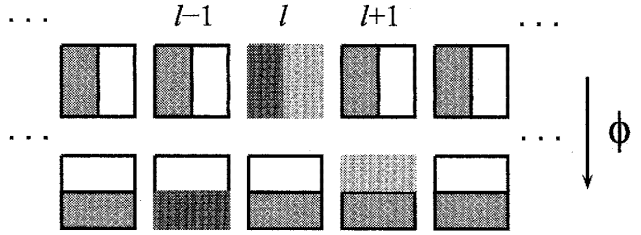

Figure 2: Schematic representation of the action of the multibaker map (2) on several cells of its phase space.

In the multibaker map, the lattice structure is kept but the Poincaré-Birkhoff map is replaced by a piecewise-linear map similar to the one of the famous baker map [4]. Several versions can be considered but the simplest one is the dyadic multibaker map:

$$(l_{t+1}, x_{t+1}, y_{t+1}) = \boldsymbol{\phi}(l_t, x_t, y_t)\,, \tag{1}$$

where

$$\boldsymbol{\phi}(l,x,y) = \begin{cases} \left(l-1, 2x, \frac{y}{2}\right)\,, & 0 \le x \le \frac{1}{2}\,, \\ \left(l+1, 2x-1, \frac{y+1}{2}\right)\,, & \frac{1}{2} < x \le 1\,, \end{cases} \tag{2}$$

with $l \in \mathbb{Z}$, $0 \leq x \leq 1$, $0 \leq y \leq 1$, and $t \in \mathbb{Z}$ [1, 2]. This map, which is schematically depicted in Fig. 2, has several features of a microscopic Hamiltonian dynamics such as the time-reversal symmetry and the property of satisfying Liouville's theorem. Indeed, the velocity inversion is performed by the involution

$$\boldsymbol{\theta}\,(l, x, y) = (l, 1-y, 1-x)\ , \tag{3}$$

which has the effect of reversing the multibaker map:

$$\boldsymbol{\phi}^{-1} = \boldsymbol{\theta} \circ \boldsymbol{\phi} \circ \boldsymbol{\theta}\,. \tag{4}$$

On the other hand, the map (2) is area preserving because its Jacobian determinant is equal to unity so that Liouville's theorem is satisfied. Moreover, the dyadic multibaker map is chaotic with a positive Lyapunov exponent equal to $\lambda = \ln 2$.

2.2 The time evolution of statistical ensembles

As in Lorentz gases, ensembles of independent particles can be transported by the multibaker map. The density $\rho(l, x, y)$ of these particles follows the Liouvillian time evolution:

$$\rho_{t+1}(l, x, y) = \hat{P}\rho_t(l, x, y)\,, \tag{5}$$

ruled by the Frobenius-Perron operator:

$$\hat{P}\rho(l, x, y) = \rho\left[\boldsymbol{\phi}^{-1}(l, x, y)\right]\ . \tag{6}$$

If a single particle is transported, $\rho_t(l, x, y)$ represents the probability density to find the particle in (l, x, y) at the time t. The number of particles in the l^{th} cell at the time t is defined by

$$N_t(l) = \int_0^1 dx \int_0^1 dy\, \rho_t(l, x, y)\,. \tag{7}$$

Since the dyadic multibaker map is expanding by a factor 2 along the x-axis, the density $\rho_t(l, x, y)$ may be supposed to become quasi uniform after a few iterations: $\rho_t(l, x, y) = \rho_t(l, y)$. As a consequence of this assumption, the numbers of particles (7) evolve in time according to

$$N_{t+1}(l) = \frac{1}{2}N_t(l+1) + \frac{1}{2}N_t(l-1)\,. \tag{8}$$

This linear equation can be solved by considering particular solutions of the form, $N_t(l) \sim \exp(ikl + st)$ to get the dispersion relation:

$$s = \ln\cos k = -\frac{k^2}{2} + O(k^4) = -\mathcal{D}\,k^2 + O(k^4)\,, \tag{9}$$

which shows the diffusive character of transport in the multibaker map with the diffusion coefficient:

$$\mathcal{D} = \frac{1}{2}\,. \tag{10}$$

Accordingly, the multibaker map defined by Eq. (2) is a model of deterministic diffusion along the infinite lattice $l \in \mathbb{Z}$.

2.3 The multibaker map connected to reservoirs

In several circumstances, diffusion is considered in finite samples connected at both ends to reservoirs at different densities, as illustrated in Fig. 3 for the Lorentz gas. A modification of the multibaker map has been proposed that describes a similar situation where the particles follow translational motions in the reservoirs [2]

$$\phi_L(l,x,y) = \begin{cases} \left(l-1, 2x, \frac{y}{2}\right), & 0 \le x \le \frac{1}{2}, \quad +1 \le l \le L+1, \\ \left(l+1, 2x-1, \frac{y+1}{2}\right), & \frac{1}{2} < x \le 1, \quad -1 \le l \le L-1, \\ (l-1, x, y), & 0 \le x \le \frac{1}{2}, \quad l \le 0 \text{ or } L+2 \le l, \\ (l+1, x, y), & \frac{1}{2} < x \le 1, \quad l \le -2 \text{ or } L \le l. \end{cases} \tag{11}$$

In this case, the diffusive motion takes place in the part of length L between both reservoirs (see Fig. 4). Therefore, the transport equation (8) holds only for $0 \le l \le L$ and boundary conditions should be taken at the reservoirs where the densities are kept constant: $N_t(-1) = \rho_-$ and $N_t(L+1) = \rho_+$ for all times $t > 0$. The stationary solution of the transport equation presents an interpolating linear profile of density in agreement with Fick's law of diffusion.

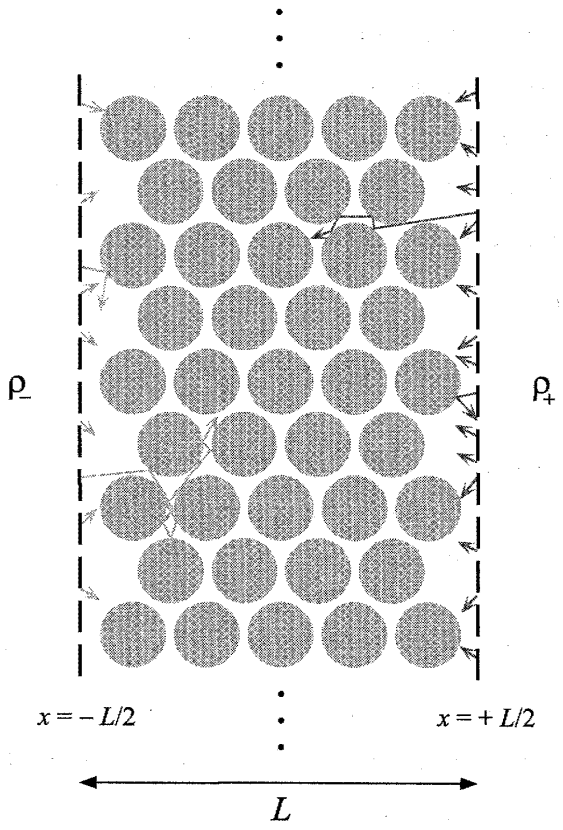

Figure 3: Slab of the hard-disk Lorentz gas in between two particle reservoirs.

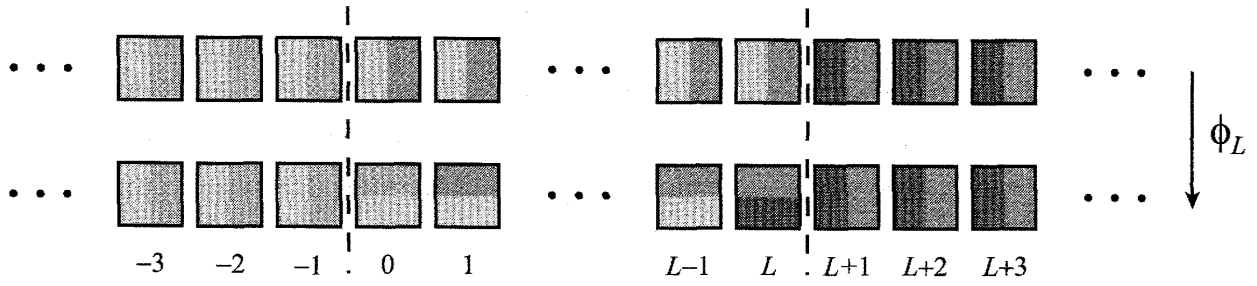

Figure 4: Finite chain of the multibaker map connected to two particle reservoirs at $l < 0$ and $L < l$.

2.4 The time evolution of cumulative functions

The inconvenience of the transport equation (8) is that it relies on the assumption that the density is uniform along the x-axis and only provides a coarse-grained description of the kinetics. A complete description is nevertheless available in terms of the cumulative functions defined as

$$F_t(l,x,y) = \int_0^x dx' \int_0^y dy'\, \rho_t(l,x',y')\,. \tag{12}$$

The advantage of the cumulative function over the density is that it is more regular and is still defined even if the density is no longer a function but a singular distribution, as it turns out to be the case in the long-time limit of Liouville's dynamics.

The time evolution of the cumulative function can be deduced from the expression (2) of the multibaker map and the definition (6) of the Frobenius-Perron operator:

$$F_{t+1}(l,x,y) = \begin{cases} F_t\left(l+1, \frac{x}{2}, 2y\right)\,, & 0 \le y \le \frac{1}{2}\,, \\ F_t\left(l+1, \frac{x}{2}, 1\right) + F_t\left(l-1, \frac{x+1}{2}, 2y-1\right) - F_t\left(l-1, \frac{1}{2}, 2y-1\right)\,, & \frac{1}{2} < y \le 1\,. \end{cases} \tag{13}$$

This equation was the starting point of the 1994 and 1995 papers with Shuichi Tasaki [1, 2]. As shown in the following sections, it allows the construction of the nonequilibrium steady states and relaxation modes of the multibaker map.

2.5 Many-body probability measures

Both aforementioned versions of the multibaker are infinite many-body systems because the dynamics takes place on infinitely many cells, $l \in \mathbb{Z}$, where infinitely many particles are transported. These particles form a gas with a finite non-uniform density extending at arbitrarily large distances. A probability measure can be introduced as a Poisson suspension [28, 29].

Let B denotes any domain of the one-body phase space $\mathcal{M} = \mathbb{Z} \otimes [0,1] \otimes [0,1]$. The domain B may belong to either one or several cells of the chain. The number of particles in the domain B is given by the measure:

$$\nu(B) = \int_B dx\, dy\, \rho(l,x,y)\,, \tag{14}$$

in terms of the particle density $\rho(l,x,y)$. The many-body phase space $\mathcal{M}^\infty$ is the direct product of infinitely many copies of the one-body phase space $\mathcal{M}$. A subset of the many-body phase space, $C_{B,n} \subset \mathcal{M}^\infty$, can be defined as a set composed of the configurations of all the particles in the system such that n particles are found in the domain $B \subset \mathcal{M}$.

The probability measure of the Poisson suspension corresponding to the measure ν is defined as

$$\mu(C_{B,n}) = \frac{[\nu(B)]^n}{n!} \exp\left[-\nu(B)\right] , \tag{15}$$

which is the probability to find n particles randomly distributed according to a Poisson distribution of average particle number equal to $\nu(B)$. For non-intersecting domains B_1 and B_2, the measure factorizes as

$$\mu(C_{B_1,n_1} \cap C_{B_2,n_2}) = \mu(C_{B_1,n_1})\,\mu(C_{B_2,n_2}) \qquad \text{if} \quad B_1 \cap B_2 = \emptyset . \tag{16}$$

With these assumptions, we can verify that the probability to find n particles in a domain $B = B_1 \cup B_2$ composed of two non-intersecting domains B_1 and B_2 respectively containing n_1 and n_2 particles is again a Poisson distribution. Indeed, the numbers n_1 and n_2 are Poissonian random variables of respective averages $\nu(B_1)$ and $\nu(B_2)$. Since $n = n_1 + n_2$, the statistical independence (16) implies that

$$\begin{aligned} \mu(C_{B,n}) &= \sum_{n_1=0}^{n} \mu(C_{B_1,n_1} \cap C_{B_2,n-n_1}) \\ &= \sum_{n_1=0}^{n} \mu(C_{B_1,n_1})\,\mu(C_{B_2,n-n_1}) = \frac{[\nu(B)]^n}{n!} \exp\left[-\nu(B)\right] , \end{aligned} \tag{17}$$

with $\nu(B) = \nu(B_1) + \nu(B_2)$. Q.E.D. As a consequence, the measure μ is normalized to unity and, therefore, defines a probability measure.

If the measure ν is invariant under the one-body dynamics $\boldsymbol{\phi}$, the probability measure μ of the Poisson suspension defines an invariant probability measure with respect to the many-body time evolution.

3 The nonequilibrium steady states

The remarkable progress carried out in the early nineties is that the solution of the Frobenius-Perron operator could be obtained at the level of the phase space [1, 2, 5, 30, 31].

In particular, the nonequilibrium steady state has been constructed in terms of the Takagi function, introduced in 1903 as an example of continuous but nondifferentiable function [32, 33]. This function has its origin in the mixing of the densities coming from the left and right reservoirs in Fig. 4. In the long-time limit, the mixing leads to a steady distribution. At almost every point in the phase space, the value of the density is either ρ_+ or ρ_-, depending on the reservoir

from which the trajectory is coming. However, the corresponding domains are intertwined on arbitarily fine scales. Indeed, the finite multibaker chain contains a fractal invariant set of trapped trajectories which cannot escape to infinity in the past or the future and where the dynamics is chaotic. The unstable manifolds of this set form the lines of discontinuities of the asymptotic density. Accordingly, the steady density presents discontinuities in the stable phase-space direction, but is smooth in the unstable direction [5, 31]. In the limit where the length L of the multibaker chain is arbitrarily large, the fractal invariant set becomes dense in phase space so that the lines of discontinuities are arbitrarily close to any phase-space point. Therefore, we should expect that the corresponding distribution becomes singular. The cumulative function (12) should be introduced in order to represent such a distribution. Indeed, the calculation of this function shows that it is composed of a singular term beside a smooth term describing the linear profile of density interpolating between both reservoirs:

$$F_\infty(l,x,y) = \rho_l\, x\, y + (\nabla\rho)\, x\, T(y)\,, \tag{18}$$

where $T(y)$ is the nondifferentiable continuous function of the singular part such that $T(0) = T(1) = 0$ [1, 2]. Since the number of particles in the l^{th} cell is given by $N_\infty(l) = F_\infty(l,1,1)$ and should obey the transport equation (8) with the boundary conditions $N_\infty(-1) = \rho_-$ and $N_\infty(L+1) = \rho_+$, the profile of density is indeed linear

$$\rho_l = (\nabla\rho)\,(l+1) + \rho_-\,, \tag{19}$$

with the gradient

$$\nabla\rho = \frac{\rho_+ - \rho_-}{L+2}\,, \tag{20}$$

in agreement with Fick's law.

On the other hand, the cumulative function (18) of the steady state obeys Eq. (13) so that the extra function should satisfy

$$T(y) = \begin{cases} \frac{1}{2}\,T(2y) + y\,, & 0 \le y \le \frac{1}{2}\,, \\ \\ \frac{1}{2}\,T(2y-1) + 1 - y\,, & \frac{1}{2} < y \le 1\,, \end{cases} \tag{21}$$

which defines the Takagi function [32, 33]. This function, which is depicted in Fig. 5, is continuous without finite derivative everywhere. Indeed, its derivative obeys

$$\frac{dT}{dy}(y) = \begin{cases} \frac{dT}{dy}(2y) + 1\,, & 0 \le y \le \frac{1}{2}\,, \\ \\ \frac{dT}{dy}(2y-1) - 1\,, & \frac{1}{2} < y \le 1\,, \end{cases} \tag{22}$$

Therefore, its derivative is given by the sum:

$$\frac{dT}{dy}(y) = \sum_{t=-1}^{-\infty} \varepsilon_t\,, \tag{23}$$

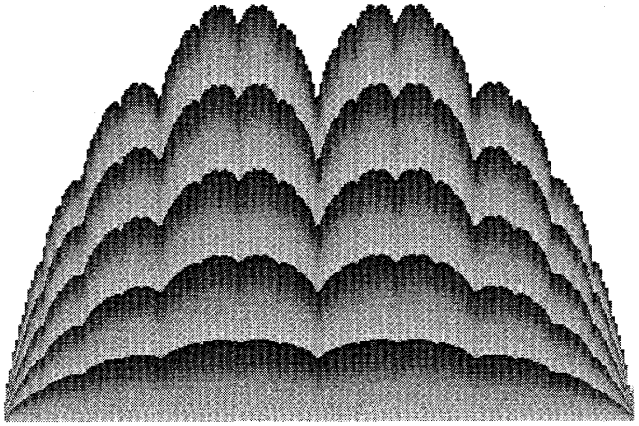

Figure 5: Multiples $xT(y)$ of the Takagi function versus the variable y, representing the singular part of the cumulative function of the nonequilibrium steady state of the dyadic multibaker map. The color changes for different values of the variable x.

with $\varepsilon_t = \pm 1$ whether the point y undergoes the jump $l \to l \pm 1$ under the t^{th} iteration of the map $\boldsymbol{\phi}$. Therefore, the sum (23) gives the reservoir from which the trajectory is coming in the remote past. However, such a sum does not converge for every sequence of ± 1 so that the Takagi function has no finite derivative everywhere. Consequently, the density of the nonequilibrium steady state

$$\rho_\infty(l,x,y) = \partial_x \partial_y F_\infty(l,x,y) = \rho_l + (\nabla\rho)\,\frac{dT}{dy}(y)\,, \tag{24}$$

is given by a singular distribution. The implications of this result are multiple.

First, it shows that the nonequilibrium steady states should not be supposed to be given by regular distributions if their construction is conceivable in the phase space of the microscopic dynamics. The fact is that this construction has been carried out for Lorentz gases, which confirms the singular character of these stationary distributions [5, 31, 34]. A direct consequence is that the density of these distributions cannot be represented in terms of a function. Instead, these distributions should be considered of Schwartz type in terms of an application from a set of smooth enough test functions $\{A(l,x,y)\}$ onto real numbers, $\langle A\,\rho_\infty\rangle = \sum_l \int dx\,dy\,A(l,x,y)\,\rho_\infty(l,x,y)$ [35, 36]. Taking the test functions, i.e. the observables, as the indicator functions of phase-space subsets such that $A(l,x,y) = 1$ if $(l,x,y) \in B$ and zero otherwise, this framework is nothing else than the usual coarse-graining procedure. In this regard, the singular character of the nonequilibrium steady states justifies coarse graining at the fundamental level.

Secondly, it is possible to calculate the time evolution of a standard coarse-grained entropy until a steady state is reached. Remarkably, this calculation shows that the entropy production

has the form expected from macroscopic laws because of the singularity of nonequilibrium steady states [5, 29, 37]. The generality of this result has been established for diffusion processes simulated by molecular dynamics [38]. The same calculation also shows that the diffusion coefficient is given by the Green-Kubo formula as expected. The novelty is that this latter appears as the statistical average of the flux of diffusive particles over the singular part of the nonequilibrium steady state. Indeed, this part is at the origin of the time integral $\int_0^{-\infty} \mathbf{v}(\Gamma_t)\, dt$ of the particle velocity back to its entrance from a reservoir, which precisely corresponds to the sum (23). Similar considerations apply to the other transport properties, as shown elsewhere [5, 30].

4 The relaxation modes of diffusion

The multibaker map can also be solved for its diffusive modes of relaxation toward the thermodynamic equilibrium state. These modes are periodic in space with wavenumber k and they decay exponentially in time with a damping rate $-s$. For the slowest modes, the corresponding distribution may be assumed to be smooth and uniform along the unstable x-direction so that their cumulative function can be taken of the following form:

$$F_t(l, x, y) = \mathrm{e}^{st}\, \mathrm{e}^{ikl}\, x\, f_k(y)\,. \tag{25}$$

Inserting in Eq. (13), the function $f_k(y)$ giving the y-dependence should satisfy the recurrence equation [3, 5]

$$f_k(y) = \begin{cases} \frac{1}{2}\, \mathrm{e}^{ik-s}\, f_k(2y)\,, & 0 \le y \le \frac{1}{2}\,, \\ \frac{1}{2}\, \mathrm{e}^{ik-s} + \frac{1}{2}\, \mathrm{e}^{-ik-s}\, f_k(2y-1)\,, & \frac{1}{2} < y \le 1\,. \end{cases} \tag{26}$$

This recurrence equation poses an eigenvalue problem for the damping rate $-s$. Indeed, if the function is evaluated at $y = 1$ and $y = 1/2$, we get the condition that $f_k(1) = 1$ and, as a consequence, the dispersion relation (9), showing the consistency of the approach. The recurrence equation (26) actually defines the so-called de Rham functions [39], which are known to be continuous but nondifferentiable for $0 < |k| < \pi/3$ [3, 5]. Related results have been obtained by other methods [40, 41]. These functions are depicted in Fig. 6 for $0 \le k < 0.7$. In the complex plane, they form fractal curves of Hausdorff dimension:

$$D_{\mathrm{H}}(k) = \frac{\ln 2}{\ln(2\cos k)} = 1 + \frac{\mathcal{D}}{\lambda}\, k^2 + O(k^4)\,, \tag{27}$$

which establishes a relationship between the diffusion coefficient $\mathcal{D} = 1/2$, the Lyapunov exponent $\lambda = \ln 2$, and the fractality of the modes [42]. This result also holds for the Lorentz gases having a positive Lyapunov exponent [43].

For $k = 0$, we recover the smooth equilibrium state. In the long-wavelength limit $k \to 0$, the diffusive modes behave as quasi stationary states and, indeed, the Takagi function (21) is

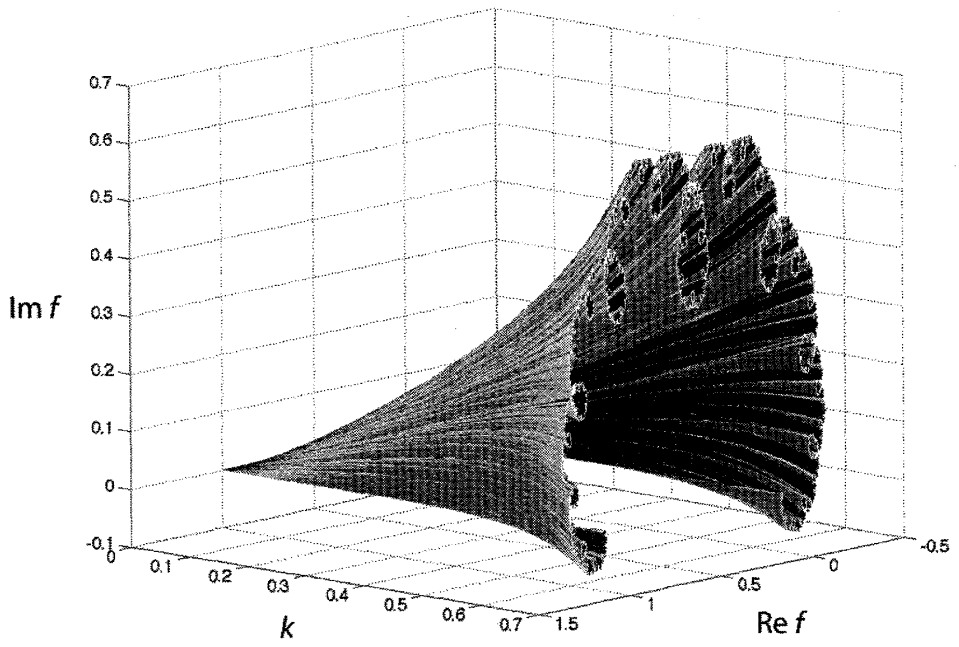

Figure 6: The diffusive modes of the multibaker map represented by their cumulative function depicted in the complex plane $(\mathrm{Re}\, f_k, \mathrm{Im}\, f_k)$ versus the wavenumber k.

recovered by taking the derivative of the de Rham function with respect to the wavenumber [1, 2, 5]

$$T(y) = -i\, \partial_k f_k(y)\Big|_{k=0} . \tag{28}$$

Since the slowest modes of diffusion are those with a vanishing wavenumber, the approach to the thermodynamic equilibrium turns out to be controlled by the Takagi function. As a consequence, the entropy production during the relaxation toward equilibrium behaves similarly as in nonequilibrium steady states and is positive because of the nondifferentiability of the Takagi function. This result applies to general diffusion processes simulated by molecular dynamics [38].

These diffusive modes are precisely the eigensolutions of the Liouvillian Frobenius-Perron equation of statistical mechanics associated with eigenvalues given by the Van Hove dispersion relation of diffusion [5, 30]. They play the same role as hydrodynamic modes in fluids [44, 45]. These eigensolutions provide a spectral decomposition of the Frobenius-Perron operator, which is valid for the forward time evolution at positive times. After completing the analysis of the multibaker, similar constructions were obtained for Lorentz gases [5, 30].

5 The time-reversal symmetry and its breaking

The multibaker map is a model for which the programme of nonequilibrium statistical mechanics can be carried out exactly and completely starting from the Liouvillian equation of motion. The nonequilibrium steady states and the relaxation modes associated with the dispersion relations

are exactly obtained, although approximations should be invoked to obtain these modes for dilute gases in kinetic theory [46, 47, 48, 49, 50]. In this regard, the analysis of the multibaker justifies the existence of these relaxation modes on a fundamental ground. Furthermore, the exact construction of these states or modes allows us to inquire about the origins of the time-reversal symmetry breaking.

For the dynamics of the multibaker map, the time-reversal transformation (3) applies the unstable manifolds which are parallel to the x-axis onto the stable manifolds parallel to the y-axis. Therefore, a distribution which is smooth along the unstable direction but singular in the stable one is transformed into another distribution which is smooth in the stable direction and singular in the unstable one. Since the stable and unstable directions are distinct in the phase space of physical observables, a distribution and its time reversal represent physically different situations, which can be distinguished by observation.

In particular, the density (24) of the nonequilibrium steady states is different from its time reversal if the gradient of concentration is non vanishing:

$$\text{out of equilibrium:} \qquad \rho_\infty(l,x,y) \neq \rho_\infty\left[\boldsymbol{\theta}(l,x,y)\right] \qquad \text{if} \quad \nabla\rho \neq 0\,; \tag{29}$$

$$\text{at equilibrium:} \qquad \rho_\infty(l,x,y) = \rho_\infty\left[\boldsymbol{\theta}(l,x,y)\right] \qquad \text{if} \quad \nabla\rho = 0\,. \tag{30}$$

At the thermodynamic equilibrium where the gradient vanishes, the density (24) is identical to its time reversal: $\rho_\infty(l,x,y) = \rho_+ = \rho_-$. In this case, the time-reversal symmetry is recovered, which justifies the principle of detailed balancing at equilibrium. However, under nonequilibrium conditions $\rho_+ \neq \rho_-$, the time-reversal symmetry is broken by the statistical distribution. There is here no contradiction with the time-reversal symmetry of the Liouvillian equation of motion because we know that the solutions of an equation may have a lower symmetry than the equation itself, which is a well-known phenomenon called spontaneous symmetry breaking in condensed-matter physics. We have here such a phenomenon for the discrete symmetry of time reversal [45].

A deeper understanding is reached by considering the relaxation modes. For the multibaker map, the complete spectral decomposition of the Frobenius-Perron operator has been constructed in terms of the Pollicott-Ruelle resonances $s_k^{(n)} = \ln\cos k - n\ln 2$ with $n = 0, 1, 2, 3, \ldots$. The time evolution of the density can be expressed as

$$\rho_t(l,x,y) = \int dk\, c_k\, \mathrm{e}^{s_k t}\, \mathrm{e}^{ikl}\, \Psi_k(y) + \cdots \tag{31}$$

where c_k is a coefficient specified by the initial density, $s_k = s_k^{(0)}$, $\Psi_k(y) = \partial_y f_k(y)$, and the dots denote typically faster contributions due to further Pollicott-Ruelle resonances with $n > 0$. Here also, the eigendistributions are smooth in the unstable direction but singular in the stable one. They are thus transformed into different distributions under the time-reversal operation (3). An

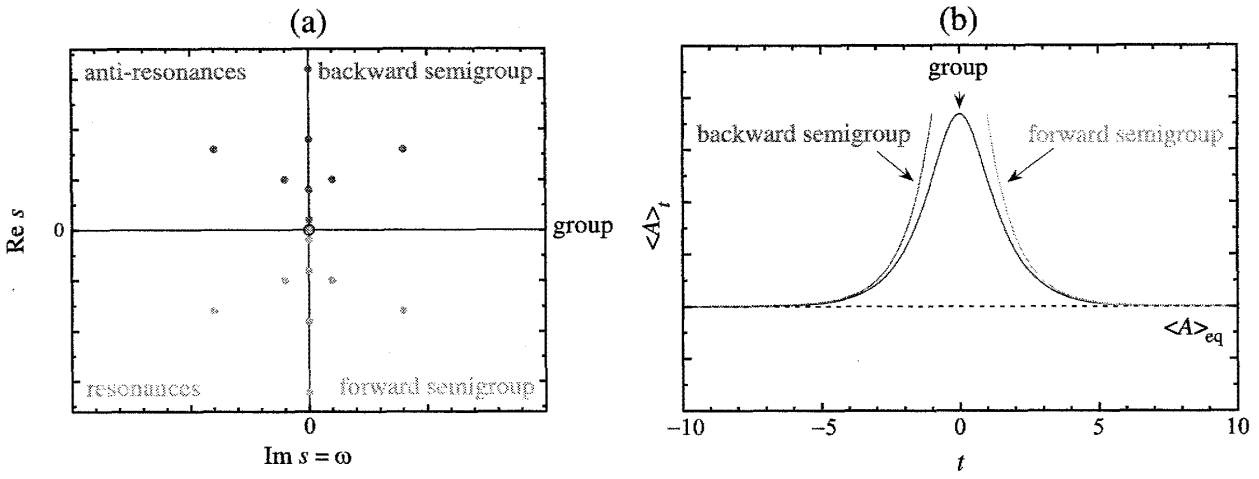

Figure 7: (a) Pollicott-Ruelle resonances and anti-resonances in the complex plane of the rate $s = -\gamma + i\omega$. (b) Time decay of the mean value of an observable A toward its equilibrium value according to the group of time evolution and asymptotic expansions of the forward and backward semigroups valid for either positive or negative times.

essential point is that the expansion (31) is obtained by analytic continuation of the evolution operator from real toward complex frequencies with a negative real part in order to pick up the contributions of the Pollicott-Ruelle resonances (see Fig. 7). In doing so, the expansion becomes limited to positive times, defining the forward semigroup. A similar analytic continuation could be carried out toward complex frequencies with a positive real part now to get the contributions of the anti-resonances. This other expansion would only be valid for negative time and would define the backward semigroup. The eigendistributions of the spectral decomposition of the backward semigroup are the time reversals of those of the forward semigroup, which are found here above. Clearly, the time evolution toward the past is stretching phase-space domains in the y-direction so that the corresponding eigendistributions should indeed be smooth in the y-direction but singular in the x-direction.

Here, we have a phenomenon of time-reversal spontaneous symmetry breaking arising when the group of time evolution is replaced by the asymptotic expansions of either the forward or backward semigroups. The representation by the group of the time evolution uses a spectral decomposition in terms of the continuous spectrum of real frequencies at $\mathrm{Re}\, s = 0$. This representation of the time evolution is valid for both positive and negative times but does not reveal the characteristic times, which are intrinsic to the dynamics. These latter ones are obtained by carrying out analytic continuations leading to the asymptotic expansions of the semigroups, which are only valid on a half-axis of time and for which the time-reversal symmetry is spontaneously broken. This symmetry breaking is the feature of all the singular distributions describing the relaxation modes and the nonequilibrium steady states. Since the singularity of these distributions is at the origin of the entropy production, a fundamental understanding of the thermodynamic

time asymmetry is here established in terms of a symmetry breaking phenomenon similar to other ones known in condensed-matter physics.

6 The current fluctuation theorem

Here, we consider the multibaker map (11) connected at its ends to two reservoirs of particles at constant densities $\rho_{\pm}$. After transients, the system reaches a steady state described by an invariant probability measure which is the Poisson suspension (15)-(16) associated with the invariant particle density $\rho_{\infty}(l, x, y)$.

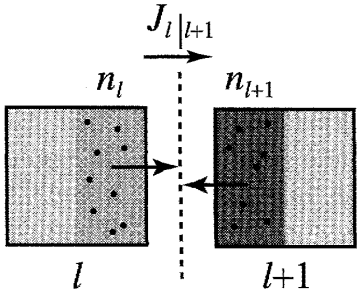

Figure 8: Schematic representation of the mechanism generating the current (32) in the multibaker map.

Between any two cells l and $l+1$ in the multibaker chain and at every time step, there is a fluctuating current from left to right, which is defined as

$$J_{l|l+1} = n_l - n_{l+1}\,, \tag{32}$$

where n_l is the random number of particles in the right-hand side of the l^{th} cell and n_{l+1} the particle number in the left-hand side of the $(l+1)^{\text{th}}$ cell (see Fig. 8).

Since the multibaker maps the right-hand side of the l^{th} cell onto the $(l+1)^{\text{th}}$ cell and the left-hand side of the $(l+1)^{\text{th}}$ cell onto the l^{th} cell, the difference between the particle numbers n_l and n_{l+1} gives the instantaneous current at the time t. In the steady state, the average values of these numbers are equal to

$$\langle n_l \rangle = \frac{\rho_l}{2}\,, \tag{33}$$

$$\langle n_{l+1} \rangle = \frac{\rho_{l+1}}{2}\,, \tag{34}$$

where ρ_l is the particle density in the l^{th} cell, which should be divided by two because the transported particles only occupy one half of each cell. Because of Eq. (19), the mean value of the current (32) thus obeys Fick's law,

$$\langle J_{l|l+1} \rangle = -\mathcal{D}\,\nabla\rho\,, \tag{35}$$

with the diffusion coefficient $\mathcal{D} = 1/2$.

Here, we are interested by the fluctuations of the current. The aforementioned numbers of particles are random variables of the following Poisson distributions:

$$P(n_l) = \frac{1}{n_l!}\left(\frac{\rho_l}{2}\right)^{n_l} \mathrm{e}^{-\frac{\rho_l}{2}}, \tag{36}$$

$$P(n_{l+1}) = \frac{1}{n_{l+1}!}\left(\frac{\rho_{l+1}}{2}\right)^{n_{l+1}} \mathrm{e}^{-\frac{\rho_{l+1}}{2}}. \tag{37}$$

Moreover, these random variables are statistically independent because they count the particles in disjoint phase-space domains for which Eq. (16) holds. Now, the problem is to deduce the probability distribution of the instantaneous current (32). For this purpose, we have the

Theorem: *If n and n' are two independent random variables of Poisson distributions with average values $\nu = \langle n \rangle$ and $\nu' = \langle n' \rangle$, their difference is distributed according to*

$$P(m = n - n') = \mathrm{e}^{-(\nu+\nu')}\left(\frac{\nu}{\nu'}\right)^{m/2} I_m\left(2\sqrt{\nu\nu'}\right), \tag{38}$$

where $m \in \mathbb{Z}$ and $I_m(z)$ is the modified Bessel function defined by [51]

$$I_m(z) = I_{-m}(z) = \left(\frac{z}{2}\right)^m \sum_{i=0}^{\infty} \frac{(z^2/4)^i}{i!\,(i+m)!}. \tag{39}$$

For $m \geq 0$, this theorem is proved as follows:

$$\begin{aligned} P(m = n - n') &= \sum_{i=0}^{\infty} P(n = i + m)\, P(n' = i) \\ &= \mathrm{e}^{-(\nu+\nu')} \sum_{i=0}^{\infty} \frac{\nu^{i+m}}{(i+m)!}\,\frac{\nu'^{i}}{i!} \\ &= \mathrm{e}^{-(\nu+\nu')}\,\nu^m \sum_{i=0}^{\infty} \frac{(\nu\nu')^i}{i!\,(i+m)!} \\ &= \mathrm{e}^{-(\nu+\nu')}\left(\frac{\nu}{\nu'}\right)^{m/2} I_m\left(2\sqrt{\nu\nu'}\right), \end{aligned} \tag{40}$$

where Eq. (39) is used with $z = 2\sqrt{\nu\nu'}$. A similar calculation holds for $m < 0$. Q.E.D.

Consequently, the probability distribution of the instantaneous current (32) is given by

$$P\left(J_{l|l+1} = m\right) = \mathrm{e}^{-(\rho_l+\rho_{l+1})/2}\left(\frac{\rho_l}{\rho_{l+1}}\right)^{m/2} I_m\left(\sqrt{\rho_l\,\rho_{l+1}}\right), \tag{41}$$

for $m \in \mathbb{Z}$. This distribution is normalized to unity and has the mean value (35).

If we compare opposite fluctuations of the current, we obtain the remarkable property that

$$\frac{P\left(J_{l|l+1} = m\right)}{P\left(J_{l|l+1} = -m\right)} = \left(\frac{\rho_l}{\rho_{l+1}}\right)^m = \mathrm{e}^{A_l\, m}, \tag{42}$$

where

$$A_l = \ln\frac{\rho_l}{\rho_{l+1}} \tag{43}$$

represents the local thermodynamic affinity driving the diffusive current out of equilibrium.

We notice that the local entropy production in the l^{th} cell is given in units of Boltzmann's constant by

$$\sigma_l = \langle J_{l|l+1} \rangle A_l = \mathcal{D}(\rho_l - \rho_{l+1}) \ln \frac{\rho_l}{\rho_{l+1}} \geq 0 \,, \tag{44}$$

which is always non-negative in agreement with the second law of thermodynamics. Moreover, in the small-gradient limit $\nabla\rho \to 0$, the local thermodynamic affinity becomes proportional to the density gradient, $A_l \simeq -\nabla\rho/\rho_l$, and we recover the expected macroscopic expression for the local thermodynamic entropy production:

$$\sigma_l \simeq \mathcal{D} \frac{(\nabla\rho)^2}{\rho_l} \geq 0 \,. \tag{45}$$

In order to obtain the current fluctuation theorem, the instantaneous current (32) should be cumulated over t successive time steps, which defines the number of particles transported from left to right during the time interval t:

$$M_t \equiv \sum_{\tau=1}^{t} J_{l|l+1}(\tau) \,. \tag{46}$$

In the steady state, the mean value of this quantity is given by

$$\langle M_t \rangle = t \, \langle J_{l|l+1} \rangle = -t \, \mathcal{D} \, \nabla\rho \,. \tag{47}$$

In phase space, the observable (46) can be expressed as the difference between two sums of numbers of particles occupying disjoint incoming domains of various sizes in the two reservoirs. According to the property (17), a sum of particle numbers in disjoint domains $\{B_i\}$ is again a Poisson distribution with the average value $\nu\left(\cup B_i\right) = \sum_i \nu(B_i)$. Since the difference of two independent Poisson distributions is distributed according to Eq. (38), we finally obtain the

current fluctuation theorem:
$$\frac{P\left(M_t = m\right)}{P\left(M_t = -m\right)} = \mathrm{e}^{A_l \, m \, t} \,, \tag{48}$$

with $l \in \mathbb{Z}$, $m \in \mathbb{Z}$, $t \in \mathbb{N}$, and the local thermodynamic affinity (43).

The current fluctuation theorem is an exact result for the multibaker map in the sense that it holds not only at long positive times but also at every time steps. It characterizes the invariant probability measure of the steady state given by the Poisson suspension (15)-(16). Furthermore, it is proved directly from the microscopic reversible area-preserving deterministic dynamics without any approximation.

7 Conclusions

With the invaluable contributions of Shuichi Tasaki, a complete and deep understanding of the multibaker map and its ergodic properties is available today. These properties also concern the

many other versions of this model. Indeed, multibaker models exist to describe diffusion not only in one spatial dimension, but also in two dimensions, in random media, and in the presence of reactions or external fields [52, 53, 54, 55, 56, 57, 58, 59, 60, 61, 62]. This latter case has been considered for volume-preserving maps with an extra energy variable [53, 54] and an equivalence was found with non-area-preserving multibaker maps, in which entropy production is associated with phase-space contraction, an issue that has been debated [63]. Quantum versions of the multibaker map have also been proposed [64].

The multibaker map is one of the simplest models of transport by diffusion for which the programme of nonequilibrium statistical mechanics has been carried out in full mathematical rigor up to the decomposition of its Liouvillian dynamics into exponentially damped hydrodynamic modes [44, 45]. The mixing dynamics of the multibaker map induces the singular character of the distributions describing the nonequilibrium steady states and the diffusive modes. Thanks to its simplicity, the multibaker map allows us to understand the origins of the time-reversal symmetry breaking and of the thermodynamic entropy production. Therefore, the study of the multibaker map has brought us insights into the ideas and techniques needed to treat more realistic systems [65]. In particular, the construction of the nonequilibrium steady states and diffusive modes has been extended to the Lorentz gases [34, 43]. Moreover, the singularity of the nonequilibrium steady states has been shown to be instrumental for the calculation of the diffusion entropy production in many-body systems simulated by molecular dynamics [38]. Furthermore, the transport property of viscosity has been studied along similar lines [66, 67].

The mathematical construction of the diffusive modes uses dynamical large-deviation properties as it is also the case for the current fluctuation theorem [18, 68]. Here, this theorem is proved for the multibaker map, directly from the deterministic dynamics without any approximation, contrary to what is done if stochastic processes are invoked. An important point is that the current fluctuation theorem concerns the many-body system of non-interacting particles described by the Poisson suspension more than the ergodic properties of the multibaker map in its one-body phase space. The current fluctuation theorem characterizes the Poisson invariant probability measure of the many-body system in some equilibrium or nonequilibrium steady state. The current fluctuation theorem is the consequence of microreversibility and the breaking of the time-reversal symmetry by the Poisson invariant probability measure out of equilibrium. The proof of this theorem for the multibaker map establishes the link with our most recent work with Shuichi Tasaki on the fluctuation theorem for currents in open quantum systems [20]. In this work, we considered open systems connected to more than two reservoirs so that the coupling between multiple currents becomes possible. This work was carried out from March 2006 until the completion of the detailed proof in June 2008 and published in April 2009. During that period, Shuichi Tasaki also thought to perform a C^*-algebraic proof of this theorem.

In conclusion, Shuichi Tasaki is leaving a deep and inspiring legacy by his fundamental contributions to the mathematical theory of irreversibility and, more generally, to condensed matter theory.

Acknowledgments. D. Andrieux thanks the F.R.S.-FNRS Belgium for financial support. This research is financially supported by the Belgian Federal Government (IAP project "NOSY").

References

[1] S. Tasaki and P. Gaspard, in: M. Yamaguti, Editor, *Towards the Harnessing of Chaos* (Elsevier Science B. V., Amsterdam, 1994) pp. 273-288.

[2] S. Tasaki, and P. Gaspard, *J. Stat. Phys.* **81**, 935 (1995).

[3] S. Tasaki and P. Gaspard, *Bussei Kenkyu Research Report in Condensed-Matter Theory* **66**, 23 (1996).

[4] P. Gaspard, *J. Stat. Phys.* **68**, 673 (1992).

[5] P. Gaspard, *Chaos, Scattering and Statistical Mechanics* (Cambridge University Press, Cambridge UK, 1998).

[6] J. R. Dorfman, *An Introduction to Chaos in Nonequilibrium Statistical Mechanics* (Cambridge University Press, Cambridge UK, 1999).

[7] M. Pollicott, *Invent. Math.* **81**, 413 (1985).

[8] M. Pollicott, *Invent. Math.* **85**, 147 (1986).

[9] D. Ruelle, *Phys. Rev. Lett.* **56**, 405 (1986).

[10] D. Ruelle, *J. Stat. Phys.* **44**, 281 (1986).

[11] J.-P. Eckmann and D. Ruelle, *Rev. Mod. Phys.* **57**, 617 (1985).

[12] P. Gaspard and G. Nicolis, *Phys. Rev. Lett.* **65**, 1693 (1990).

[13] D. J. Evans, E. G. D. Cohen, and G. P. Morriss, *Phys. Rev. Lett.* **71**, 2401 (1993).

[14] P. Gaspard and F. Baras, *Phys. Rev. E* **51**, 5332 (1995).

[15] J. R. Dorfman and P. Gaspard, *Phys. Rev. E* **51**, 28 (1995).

[16] P. Gaspard and J. R. Dorfman, *Phys. Rev. E* **52**, 3525 (1995).

[17] G. Gallavotti and E. G. D. Cohen, *Phys. Rev. Lett.* **74**, 2694 (1995).

[18] D. Andrieux and P. Gaspard, *J. Stat. Mech.: Th. Exp.* P01011 (2006).

[19] K. Saito and Y. Utsumi, *Phys. Rev. B* **78**, 115429 (2008).

[20] D. Andrieux, P. Gaspard, T. Monnai, and S. Tasaki, *New J. Phys.* **11**, 043014 (2009).

[21] M. Esposito, U. Harbola, and S. Mukamel, *Rev. Mod. Phys.* **81**, 1665 (2009).

[22] Y. Utsumi, D. S. Golubev, M. Marthaler, K. Saito, T. Fujisawa, and G. Schön, *Phys. Rev. B* **81**, 125331 (2010).

[23] S. Nakamura, Y. Yamauchi, M. Hashisaka, K. Chida, K. Kobayashi, T. Ono, R. Leturcq, K. Ensslin, K. Saito, Y. Utsumi, and A. C. Gossard, *Phys. Rev. B* **83**, 155431 (2011).

[24] M. Campisi, P. Hänggi, and P. Talkner, *Rev. Mod. Phys.* **83**, 771 (2011).

[25] H. A. Lorentz, *Proc. Roy. Acad. Amst.* **7**, 438, 585, 684 (1905).

[26] L. A. Bunimovich, and Ya. G. Sinai, *Commun. Math. Phys.* **78**, 247, 479 (1980).

[27] A. Knauf, *Commun. Math. Phys.* **110**, 89 (1987); *Ann. Phys. (N. Y.)* **191**, 205 (1989).

[28] I. P. Cornfeld, S. V. Fomin, and Ya. G. Sinai, *Ergodic Theory* (Springer, Berlin, 1982).

[29] P. Gaspard, *J. Stat. Phys.* **88**, 1215 (1997).

[30] P. Gaspard, *Phys. Rev. E* **53**, 4379 (1996).

[31] P. Gaspard, *Physica A* **240**, 54 (1997).

[32] T. Takagi, *Proc. Phys. Math. Soc. Japan Ser. II* **1**, 176 (1903).

[33] M. Hata and M. Yamaguti, *Jpn. J. Appl. Math.* **1**, 183 (1984).

[34] P. Gaspard, *Int. J. Mod. Phys. B* **15**, 209 (2001).

[35] N. Dunford and J. T. Schwartz, *Linear operators*, Vols. I-III (Interscience-Wiley, New York, 1958, 1963, 1971).

[36] I. Gel'fand and G. Shilov, *Generalized Functions*, Vol. 2 (Academic Press, New York, 1968).

[37] T. Gilbert, J. R. Dorfman, and P. Gaspard, *Phys. Rev. Lett.* **85**, 1606 (2000).

[38] J. R. Dorfman, P. Gaspard, and T. Gilbert, *Phys. Rev. E* **66**, 026110 (2002).

[39] G. de Rham, *Rend. Sem. Mat. Torino* **16**, 101 (1957).

[40] H. H. Hasegawa and D. J. Driebe, *Phys. Rev. E* **50**, 1781 (1994).

[41] D. J. Driebe, *Fully Chaotic Maps and Broken Time Symmetry* (Kluwer, Dordrecht, 1999).

[42] T. Gilbert, J. R. Dorfman, and P. Gaspard, *Nonlinearity* **14**, 339 (2001).

[43] P. Gaspard, I. Claus, T. Gilbert, and J. R. Dorfman, *Phys. Rev. Lett.* **86**, 1506 (2001).

[44] D. Forster, *Hydrodynamic Fluctuations, Broken Symmetry, and Correlation Functions* (Benjamin/Cummings, Reading, 1975).

[45] P. Gaspard, *Adv. Chem. Phys.* **135**, 83 (2007).

[46] J. O. Hirschfelder, C. F. Curtiss, and R. B. Bird, *Molecular Theory of Gases and Liquids* (Wiley, New York, 1954).

[47] R. Balescu, *Equilibrium and Nonequilibrium Statistical Mechanics* (Wiley, New York, 1975).

[48] P. Résibois and M. De Leener, *Classical Kinetic Theory of Fluids* (Wiley, New York, 1977).

[49] J.-P. Boon and S. Yip, *Molecular Hydrodynamics* (Dover, New York, 1980).

[50] E. G. D. Cohen, I. M. de Schepper, and M. J. Zuilhof, *Physica B* **127**, 282 (1984).

[51] M. Abramowitz and I. A. Stegun, *Handbook of Mathematical Functions* (Dover, New York, 1972).

[52] T. Tél, J. Vollmer, and W. Breymann, *Europhys. Lett.* **35**, 659 (1996).

[53] S. Tasaki and P. Gaspard, *Theoretical Chemistry Accounts* **102**, 385 (1999).

[54] S. Tasaki and P. Gaspard, *J. Stat. Phys.* **101**, 125 (2000).

[55] G. Radons, *Festkörperprobleme/Advances in Solid State Physics* **38**, 339 (1999).

[56] T. Tél and J. Vollmer, *Entropy Balance, Multibaker Maps, and the Dynamics of the Lorentz gas*, in: D. Szász, Editor, *Hard Ball Systems and the Lorentz Gas* (Springer-Verlag, Berlin, 2000) pp. 367-418.

[57] J. Vollmer, T. Tél, and L. Mátyás, *J. Stat. Phys.* **101**, 79 (2000).

[58] J. Vollmer, *Phys. Rep.* **372**, 131 (2002).

[59] P. Gaspard and R. Klages, *Chaos* **8**, 409 (1998).

[60] I. Claus and P. Gaspard, *J. Stat. Phys.* **101**, 161 (2000).

[61] I. Claus and P. Gaspard, *Physica D* **168-169**, 266 (2002).

[62] P. Gaspard and I. Claus, *Phil. Trans. Roy. Soc. London A* **360** (2002).

[63] R. Klages, *Microscopic Chaos, Fractals and Transport in Nonequilibrium Statistical Mechanics* (World Scientific, New Jersey, 2007).

[64] D. K. Wojcik and J. R. Dorfman, *Phys. Rev. E* **66**, 036110 (2002).

[65] P. Gaspard, G. Nicolis, and J. R. Dorfman, Physica A **323**, 294 (2003).

[66] L. Mátyás, T. Tél, and J. Vollmer, *Phys. Rev. E* **64**, 056106 (2001).

[67] S. Viscardy and P. Gaspard, *Phys. Rev. E* **68**, 041204 (2003).

[68] D. Andrieux and P. Gaspard, *J. Stat. Phys.* **127**, 107 (2007).